PROCEEDINGS B

royalsocietypublishing.org/journal/rspb

Research

Cite this article: Kocáková K, Silvestro D, Mathes GH, Villafaña JA, Pimiento C. 2025 Global extinction events and persistent age-dependency in sharks and rays over the past 145 million years. *Proc. R. Soc. B* **292**: 20252272.
https://doi.org/10.1098/rspb.2025.2272

Received: 11 September 2025
Accepted: 30 October 2025

Subject Category:
Palaeobiology

Subject Areas:
evolution, palaeontology

Keywords:
age-dependent extinction, diversification, extinctions, Neoselachii, sharks

Authors for correspondence:
Kristína Kocáková
e-mail: kocakova.kristina@gmail.com
Daniele Silvestro
e-mail: daniele.silvestro@bsse.ethz.ch
Catalina Pimiento
e-mail: c.pimiento@swansea.ac.uk

Electronic supplementary material is available online at https://doi.org/10.6084/m9.figshare.c.8142777.

THE ROYAL SOCIETY PUBLISHING

Global extinction events and persistent age-dependency in sharks and rays over the past 145 million years

Kristína Kocáková[1], Daniele Silvestro[2,3,4], Gregor Hans Mathes[1,5], Jaime Andres Villafaña[6] and Catalina Pimiento[1,7]

[1]Department of Paleontology, University of Zurich, 8006 Zurich, Switzerland
[2]Department of Biosystems Science and Engineering, ETH Zurich, 4056 Basel, Switzerland
[3]Department of Biological and Environmental Science and Gothenburg Global Biodiversity Centre, University of Gothenburg, Gothenburg 413 19, Sweden
[4]Swiss Institute of Bioinformatics, CH 4056 Basel, Switzerland
[5]Chair of Physical Geography, University of Passau, Passau, Bavaria HF93 44, Germany
[6]Departamento de Ecología, Universidad Católica de la Santísima Concepción, Concepción 4090541, Chile
[7]Department of Biosciences, Swansea University, Swansea SA2 8PP, UK

KK, 0000-0002-2270-8435; DS, 0000-0003-0100-0961; GHM, 0000-0002-2788-1173; JAV, 000-0002-6441-9025; CP, 0000-0002-5320-7246

Understanding extinction mechanisms, including what traits make some species more vulnerable than others, is key in a changing world. It has been proposed that species' age predicts extinction risk. However, our understanding of age-dependent extinction (ADE) remains unresolved, with positive and negative trends being modelled only as mutually exclusive, and rarely across clade-specific diversification trajectories. Here, we reconstruct the global diversification trajectory of neoselachians (modern sharks and rays) over the past 145 Myr to assess ADE using a new model that allows positive and negative trends to co-occur. We recovered a dynamic diversification trajectory, including four previously undetected extinction events, the most significant in the Eocene–Oligocene. Negative ADE was consistently found over time, with young species, especially those younger than 4 Myr, being more vulnerable. Our results suggest that neoselachians have been more susceptible to extinction than previously recognized, with age being a consistent intrinsic predictor of their vulnerability through deep time.

1. Introduction

What factors predict extinction risk is a long-standing question in evolutionary biology research. The age of a taxon, i.e. the time elapsed since origination, has been proposed as a potential predictor of extinction risk (e.g. [1–4]). While the traditional view is that under the Law of Constant Extinction [5] a species' probability of going extinct is independent of its age [6], more recent studies have found evidence of age-dependent extinction (ADE) in different clades [2,3,7–11]. When present, ADE can manifest as positive or negative, representing contrasting extinction dynamics. Positive ADE indicates a strong extinction selectivity against long-lived taxa, which can be explained by the loss of fitness due to the accumulation of deleterious mutations over time, as well as the prevalence of evolutionary stasis, which can diminish species' ability to adapt to environmental changes [6,12]. Negative ADE, on the other hand, indicates extinction selectivity against short-lived taxa and has been proposed to be the result of limited evolutionary 'experience' owing to small population size, narrow geographical range, competition with already established taxa, and/or specialist ecologies [13–18]. Together, these

perspectives suggest that the relationship between extinction risk and taxon age is complex, with both positive and negative ADE being plausible under different evolutionary and ecological conditions.

Indeed, empirical studies exploring ADE have reported variation among clades, taxonomic ranks and diversification trajectories. For instance, positive ADE has been found in conodonts [6], trilobites [6] and North American mammals [2], whereas negative ADE has been observed in bryozoans [19], ammonoids [7], rudists [20] and mammalian carnivores [3]. Furthermore, ADE can vary across taxonomic ranks, with the theoretical expectation that even if extinction risk is age-independent (i.e. neutral ADE) at the species level, apparent age-dependence will emerge at higher taxonomic ranks [21]. However, empirical comparisons of ADE at different taxonomic ranks have revealed contrasting patterns—ruminant mammals have shown negative ADE at the species level and age-independence at the genus level [10], and trilobites have shown positive ADE at both levels [6]. Finally, ADE patterns have been shown to vary across diversification trajectories (e.g. times of constant or elevated extinction rates) in graptolites, with negative ADE found during times of constant extinction rates, neutral ADE during times of elevated extinction, and positive ADE during mass extinctions [8]. Overall, the varied ADE patterns found empirically underscore the challenge of drawing general conclusions, motivating closer examination of the limitations that have shaped existing studies.

Although evidence for ADE is accumulating, in our view our understanding has been limited by three main factors. First, most ADE studies to date have been restricted to well preserved taxa, or fossils with precisely resolved ages (e.g. [1–3,22]). This taxonomic restrictiveness, which potentially biases our understanding of ADE, has arisen from the methodologies currently available, which have limited power to account for preservation and sampling biases, as well as for large age uncertainties [3,6]. Second, even though it has been proposed that ADE patterns vary across diversification trajectories [23], it has rarely been assessed during periods of elevated extinction. Instead, most studies have focused on periods of constant extinction [3,10], or across global mass extinctions [20,22,24,25]. This can be problematic because clades can have contrasting responses to mass extinctions [26], with some going completely extinct, e.g. non-avian dinosaurs throughout the Cretaceous/Palaeogene (K/Pg); some only declining, e.g. birds; and others remaining unaffected, e.g. crocodilians [27–29]. Finally, ADE has generally been modelled under the assumption that positive and negative trends are mutually exclusive. This view stems from our understanding of survivorship curves, whereby most individuals in a population die either old, young, or in rare cases, randomly [30]. While this is the case for most biological populations, it is possible for positive and negative ADE to take place together over evolutionary timescales, with extinction risk being high for *both* young species (e.g. owing to small initial population or range sizes) and old species (e.g. owing to lack of adaptability to new environmental conditions). Whether or not this occurs in nature remains to be tested. In sum, ADE can be the result of complex processes, and its study requires approaches that can (i) broaden the taxonomic scope by accounting for age uncertainty in fossil occurrences, (ii) evaluate variation across clade-specific diversification trajectories (e.g. constant and elevated extinction), and (iii) capture the potential coexistence of both positive and negative ADE trends.

The monophyletic clade Neoselachii—modern sharks, rays and skates and their extinct relatives—represents an ideal model to advance our understanding of extinction mechanisms, including age-dependency [31,32]. Their rich fossil record spans at least 250 Myr and is abundant, taxonomically well resolved and globally distributed [31,33,34]. Furthermore, neoselachians exhibit remarkable morphological and ecological diversity, having habitats from brackish waters and coastal areas to the open ocean, ecologies encompassing generalists and specialists, trophic positions ranging from planktivores to apex predators, and body sizes spanning from mere centimetres to 21 m [35–42]. As a long-lived clade with diverse ecological roles in marine systems worldwide, neoselachians have experienced significant biotic and environmental changes. These dynamics likely resulted in varied longevities, stressor responses and diversification trajectories.

Previous studies have investigated neoselachian diversification trends through deep time. However, this has generally been done using high taxonomic levels (e.g. genera or families), or within regions, time periods or shark orders [25,43–50]. Despite these constraints, existing studies have provided valuable insights, suggesting two main global extinction events, the most catastrophic during the K/Pg (*ca* 66 Ma), and a moderate, yet significant event in the Plio-Pleistocene ([25], 5.33–0.01 Ma; [43,46,47,49–51]). An extinction event in the early Miocene (*ca* 23 Ma) has also been identified, although it appears to have only affected pelagic taxa [52]. Recent research further examined ADE in neoselachians throughout the K/Pg and within mackerel sharks (order Lamniformes) at the species level. At the K/Pg, ADE patterns were found to vary across taxonomic levels and geological stages, with neutral ADE found in the Turonian–Maastrichtian (93.90–72.10 Ma), Palaeocene (66–56 Ma), and when analysing rays and skates separately; and positive ADE found in the Maastrichtian (72.10–66 Ma; [49]). In mackerel sharks, negative ADE has been observed in medium and large species, and neutral ADE in their small counterparts [25]. Despite these advances, our understanding of neoselachian extinction mechanisms is still limited, with no global analysis of their diversification trajectories or ADE across long geological timescales to date. This gap is striking given their extensive longevity and geographical distribution [31,33], but it reflects the lack of comprehensive compendia of global fossil occurrences spanning long timescales. Nevertheless, a compilation of the neoselachian fossil record is now available, which includes over 20 000 fossil occurrences mostly identified to the species level, covering every continent and spanning the past 145 Myr [34]. This resource provides an unprecedented opportunity to investigate the deep-time diversification trajectories of this entire clade, addressing critical knowledge gaps about their extinction mechanisms, including the role of species' age in their extinction risk.

Here, we used the new compilation of neoselachian fossil occurrences [34] to reconstruct their diversification trajectories over the past 145 Myr and assess ADE. To do so, we first estimate extinction, speciation and net diversification rates over time using PyRate, a Bayesian approach that accounts for multiple biases in the fossil record [53,54]. Then, we model ADE across different extinction regimes (i.e. periods of constant, moderate and intense extinction) using ADE-NN, a deep learning neural network that allows estimating age-dependency under dynamic diversification trajectories, while permitting the use of occurrences with poor age resolution [4]. We further develop this framework by replacing the previous classification approach

with one that allows estimating the strength and direction of ADE as interpretable quantitative parameters, thereby enabling both negative and positive ADE to act simultaneously. Our results reveal previously undetected extinction events in the neoselachian evolutionary history and persistent age-dependency across extinction regimes, strongly suggesting that age is an intrinsic predictor of neoselachian extinctions through deep time. Overall, by broadening both the taxonomic scope and methodological toolkit, our study advances understanding of ADE and its role in shaping macroevolutionary patterns.

2. Results and discussion

(a) 145 Myr reconstruction of neoselachian diversification trajectories

We estimated extinction, origination and net diversification rates of neoselachians over the past 145 Myr using PyRate, a Bayesian framework that estimates speciation and extinction rates and their temporal dynamics using fossil occurrences [54]. This method accounts for preservation and sampling biases, while simultaneously inferring taxon-specific times of speciation and extinction (see §3). Here, we quantified the background rates as the harmonic mean across the 145 Myr period. Periods of significant extinction and origination were identified when the rates were inferred to be at least three times higher than background rates, with their start and end points corroborated based on the timing of significant rate shifts (electronic supplementary material, figure S1). While our main analyses are based on the global assemblage at the species level and excluding singletons, we performed additional analyses at the genus level and including singletons for comparison (electronic supplementary material, figures S2 and S3). Furthermore, in order to evaluate the robustness of our findings, we carried out additional analyses using the *divDyn* R package to estimate *per capita* diversification rates for comparison (electronic supplementary material, figures S4 and S5; [55]).

Reconstruction of neoselachian extinction rates over the past 145 Myr revealed six periods of elevated extinction (figure 1a). To establish extinction regimes, we categorized these periods as either moderate (i.e. rates ≥3 times the background, estimated to be 0.02 events per lineage per million years; see §3) or intense (rates ≥6 times the background). Time intervals not meeting these thresholds were considered constant extinction periods. Moderate extinction periods took place during the (i) mid-Cenomanian–early Campanian (95.71–83.31 Ma) and (ii) Palaeocene–early Eocene (65.79–55.89 Ma; electronic supplementary material, table S1; figure 1a). Intense extinctions occurred at the (iii) Campanian/Maastrichtian (73.40–71.90 Ma), (iv) K/Pg (66.60–65.79 Ma), (v) late Eocene–early Oligocene (38.58–33.57 Ma) and (vi) late Pliocene–Pleistocene (3.65–0.01 Ma). Intense extinction periods were, on average, shorter (mean duration = 2.74 Myr) than moderate periods (mean duration = 11.10 Myr). Among them, K/Pg exhibited the highest maximum rate and the shortest duration (0.88 events per lineageper million years; 0.81 Myr), whereas the late Eocene–early Oligocene lasted the longest and displayed the third highest maximum rate (0.36 events per lineage per million years; 5.01 Myr; electronic supplementary material, table 1).

Overall, our results identify multiple periods of elevated extinction for neoselachians over the past 145 Myr, including four previously unknown extinction periods (i.e. mid-Cenomanian–early Campanian, Campanian/Maastrichtian, Palaeocene–early Eocene, late Eocene–early Oligocene), while also confirming the K/Pg and the Plio-Pleistocene events, which had been previously documented using different [43] and similar approaches [49,51]. The intensity of the K/Pg event, however, contrasts with previous analysis reporting maximum extinction rates around two times higher than those found here [49]. We attribute this discrepancy to differences in the data—while the previous study used 2560 fossil occurrences, our study contains 6152 fossil occurrences for the same time period (100.5–56 Ma). Regardless, the K/Pg remains the extinction event with the highest rates for neoselachians (electronic supplementary material, table S1; figure 1a; [43,49,56]). The newly identified preceding event in the Campanian/Maastrichtian further suggests that the K/Pg event likely affected an already depleted neoselachian diversity (figure 1a). This supports the hypothesis that marine vertebrates, including neoselachians, experienced prolonged extinction pressures before the Chicxulub impact [49,57] (but see [58]). Additionally, we identify an extinction event in the late Eocene–early Oligocene, which was the longest period of intense extinction identified here (electronic supplementary material, table S1). Although newly discovered for the entire clade, this period has been previously recognized as a time of elevated extinction for the shark orders Lamniformes and Carcharhiniformes [48,49] and has been regarded as the most significant interval after the K/Pg (e.g. [59]).

Our finding of an extinction event in the Plio-Pleistocene further aligns with previous analyses of the Cenozoic, which reported elevated extinction rates for neoselachian genera during this time [47,51]. Notably, the neoselachian extinction event we uncover here appears to have originated in the middle Miocene, as our results show above-background extinction rates starting around *ca* 16 Ma. These findings suggest that neoselachians likely sustained high extinction rates throughout the late Cenozoic (figure 1a). This is unlikely to be the result of the Pull of the Recent, given that the neoselachian fossil record does not display this pattern (electronic supplementary material, figure S6; [60]). Equally, this is unlikely to be a result of the fossil record being poorer towards the Recent, as PyRate accounts for differences in preservation (figure 1; electronic supplementary material, figures S4 and S6; [61]). Moreover, PyRate takes into consideration the number of extant taxa in the dataset (n = 132), further preventing artificial inflation of extinction rates towards the Recent [61].

Notably, our analyses did not recover an extinction event previously reported in the early Miocene, *ca* 19 Ma [52], which we attribute to differences in taxonomic and geographical scope. While our study was based on a global dataset of tooth occurrences identified at the species level [34], the previous study was based on dermal denticles assigned to morphospecies and collected from oceanic samples from the Pacific [52]. As a result, our study predominantly reflects global extinction events, likely from coastal areas, whereas the early Miocene event appears to have affected only pelagic species. Taken together, these findings provide a more nuanced understanding of neoselachian extinction trajectories, revealing new extinction events over the last 145 Myr, thereby underscoring their high vulnerability through time.

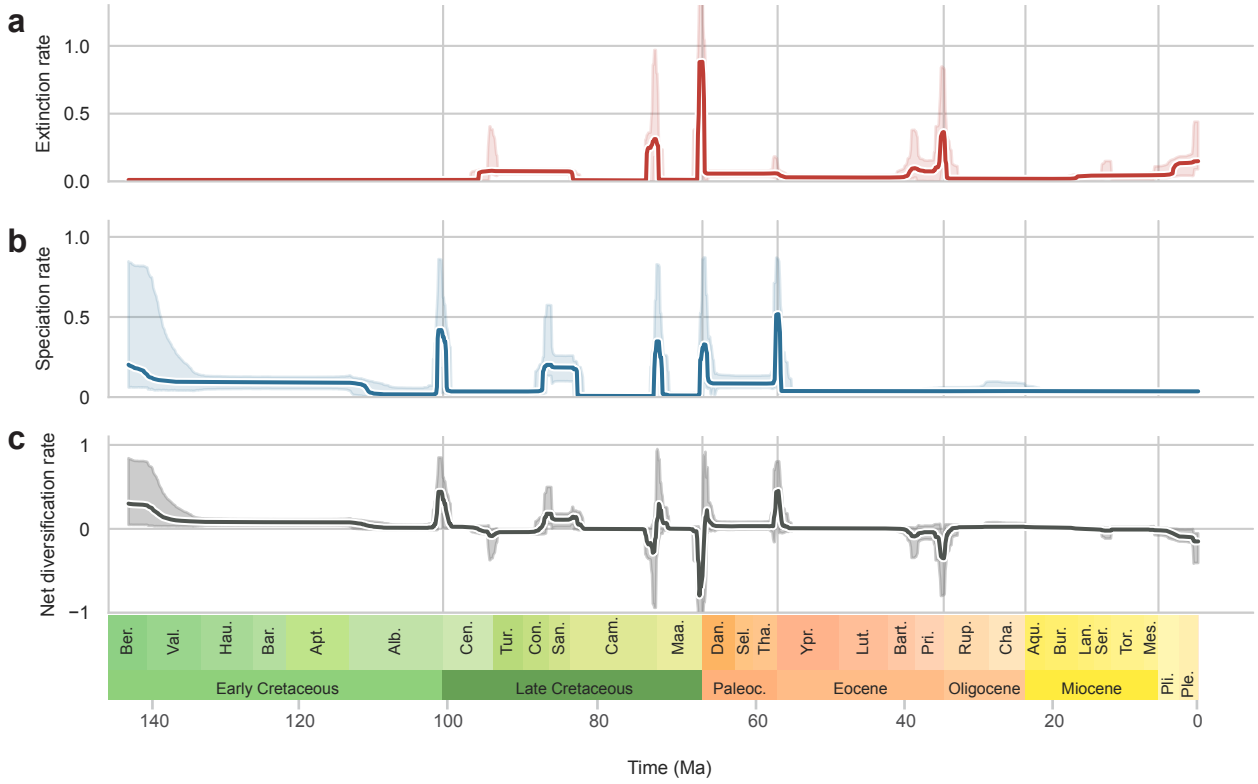

Figure 1. Diversification trajectories of neoselachian species global assemblage from the Early Cretaceous to the Pleistocene. (a) Extinction, (b) speciation and (c) net diversification rates. Solid lines represent the mean posterior rates and shaded areas the 95% CIs. Net diversification represents the difference between extinction and speciation rates. Abbreviations: Pli. = Pliocene, Ple. = Pleistocene, Ber. = Berriasian, Val. = Valanginian, Hau. = Hauterivian, Bar. = Barremian, Apt. = Aptian, Alb. = Albian, Cen. = Cenomanian, Tur. = Turonian, Con. = Coniacian, San. = Santonian, Cam. = Campanian, Maa. = Maastrichtian, Dan. = Danian, Sel. = Selandian, Tha. = Thanetian, Ypr. = Ypresian, Lut. = Lutetian, Bart. = Bartonian, Pri. = Prianonian, Rup. = Rupelian, Cha. = Chattian, Aqu. = Aquitanian, Bur. = Burdigalian, Lan. = Langhian, Ser. = Serravalian, Tor. = Tortonian, Mes. = Messinian.

We identified six periods of elevated speciation relative to background rates (0.03 events per lineage per million years), all taking place before the Eocene. The first was a prolonged period of mild speciation, spanning the majority of the Early Cretaceous up to the early Albian (145–112.23 Ma; figure 1b). This was followed by a sharp spike at the Albian/Cenomanian (101.22–100.12 Ma), prior to the first extinction event (figure 1b). All subsequent speciation periods coincided with times of elevated extinction: late Coniacian–early Campanian (87.21–82.70 Ma); Campanian/Maastrichtian (72.40–71.39 Ma); K/Pg (66.17–64.69 Ma); and Palaeocene–early Eocene (65.49–55.59 Ma), which displays the highest speciation rates across the 145 Myr period (electronic supplementary material, table S1; figure 1b).

Net diversification was generally positive throughout most of the Cretaceous, with a prolonged period of slightly positive rates in the Early Cretaceous (145–111.34 Ma) followed by a spike in the Albian/Cenomanian (101.42–99.72 Ma) and the Coniacian–early Campanian (87.11–82.61 Ma). This generally positive interval was briefly interrupted by a mild decrease at the Cenomanian/Turonian (94.42–93.62 Ma). Subsequently, there were two short periods of fast turnover, whereby sudden drops were followed by rapid spikes (i.e. late Campanian–Campanian/Maastrichtian (73.60–70.80 Ma) and K/Pg–early Danian (66.69–64.99 Ma)). The last spike took place at the Palaeocene/Eocene (56.49–55.49 Ma). Afterwards, neoselachian net diversification remained largely constant and near-zero, although there were two notable drops in the late Eocene–early Oligocene (38.28–33.37 Ma) and the late Pliocene–Pleistocene (3.15–0.01 Ma; figure 1c; electronic supplementary material, table S1).

Our speciation and net diversification reconstructions indicate that the global neoselachian evolutionary history has been highly dynamic, marked by high speciation during the Early Cretaceous, significant turnover during the Late Cretaceous and Palaeocene, and stagnating or negative net diversification thereafter (figure 1b,c).

Complementary analyses indicate that the diversification trajectories uncovered here are robust. For instance, analyses including singletons show similar patterns (electronic supplementary material, figure S3). Furthermore, complementary analyses using traditional methods yielded broadly consistent results (figure 1; electronic supplementary material, figures S4 and S5). Indeed, *per capita* diversification rates across geological stages estimated using the *divDyn* R package (see §3; [55]) indicate elevated extinction rates in the Cenomanian, Turonian, Campanian, Maastrichtian, Danian, Priabonian and from the mid-Miocene onwards, consistent with our main results. Nevertheless, it is worth noting that the *per capita* diversification rates also showed some differences, including: (i) elevated extinction rates from the Berriasian to the Hauterivian; (ii) high speciation rates during early stages of the Early Cretaceous; and (iii) extremely high extinction rates and low net diversification in the Plio-Pleistocene (electronic supplementary material, figures S4 and S5). These discrepancies likely rise from PyRate's ability to account for preservation and sampling bias [61]. For instance, the fossil-poor Pleistocene (electronic supplementary material, figure S6) inflates the *per capita* extinction rates beyond those of the K/Pg, whereas PyRate scales these rates based on

preservation intensity. Overall, our results are broadly consistent across approaches, with the remaining differences reflecting PyRate's correction for sampling and preservation biases [61].

The ability of PyRate to account for multiple biases in the fossil record also explains why the diversification patterns uncovered here are unlikely to be artefacts of age resolution of fossil occurrences or sampling intensity. Although many extinction and speciation events described here occur at boundaries between geological stages or epochs, this is unlikely to be a dating artefact because we randomly resampled fossil ages within their stratigraphic ranges (see §3). In addition, rate shifts were estimated along a continuous timescale rather than being constrained by stratigraphic boundaries, minimizing temporal bias. Finally, although PyRate has been argued to overestimate the frequency of rate shifts in well sampled time intervals [62], this does not appear to affect our results, as the estimated shifts do not systematically align with the best-sampled intervals (electronic supplementary material, figures S1 and S6). Altogether, this indicates that the trajectories we identify reflect genuine biological signals rather than statistical artefacts.

Analyses at the genus level revealed trajectories broadly consistent with those found at the species level, although less heterogeneous. For instance, only two extinction events were identified—K/Pg (66.5–65.8 Ma) and Eocene/Oligocene (34.1–33.8 Ma; electronic supplementary material, figure S2). As with our species-level results, the extinction rates recovered during the K/Pg were 2.8 times lower than previously estimated [49], which we attribute to differences in the data used (i.e. while the previous study used 3218 occurrences for genus-level analyses, we used 8814 for the same time interval). Nevertheless, the K/Pg remains the most intense extinction period in neoselachian genera. The consistent recovery of elevated extinction rates across both species and genus levels at the K/Pg and Eocene/Oligocene suggests that these were exceptionally severe. Overall, our genus-level results highlight that neoselachian diversification dynamics vary across taxonomic levels, with genera displaying more stable trajectories. These findings underscore the value of species-level analyses in uncovering intricate extinction patterns that may remain obscured at coarser taxonomic resolutions.

Taken together, our reconstruction of neoselachian diversification over the past 145 Myr reveals a dynamic evolutionary history, marked by six global extinction events, four of them previously unknown. While neoselachians experienced substantial diversification during the Cretaceous, the last 56 Myr have been far less favourable, with prolonged vulnerability. The K/Pg stands out for its elevated extinction rates but also heightened speciation, resulting in rapid turnover. Thus, although this event was impactful, it may not have been as catastrophic for neoselachian diversity as previously assumed (figure 1). Conversely, the late Eocene–early Oligocene and, to a lesser extent, the Plio-Pleistocene sustained elevated extinction rates and constant but low speciation rates, resulting in a negative net diversification without recovery (figure 1b, c). This contrasts with earlier extinction events, which were all followed by immediate increase in speciation rates (figure 1). Based on these global diversification patterns, we propose that the most significant extinction event for neoselachians occurred during the late Eocene–early Oligocene. These global patterns were broadly corroborated by traditional methods (electronic supplementary material, figure S4), and the analyses at the genus level confirmed key extinction periods but revealed more stable trajectories.

(b) Age-dependent extinction

We assessed whether global neoselachian extinctions are age-dependent through the past 145 Myr. To do so, we used the ADE-NN method [4], which employs simulations and a neural network to infer ADE patterns from fossil occurrences. Here, we updated the original method to incorporate scenarios with mixed types of ADE effects (figure 2). We first identified 10 time bins corresponding to different extinction regimes. Then, for each, we estimated the type of ADE, its parameters and the root mean square error interval (RMSE, see §3). We determined the type of ADE based on the position of the Weibull distribution shape parameter (herein, estimated position of age-dependency). The null expectation is a random extinction process, whereby the longevities of extinct taxa are exponentially distributed, which is equivalent to a position of age-dependency around 1, indicating age-independency or neutral ADE (ADE0; figure 2). Deviations from 1 reflect changes in the longevity distribution, consistent with extinction rates varying as a function of species' age [3]. Thus, an estimated position crossing 1 in either direction indicates age-dependency, with negative ADE denoted by an estimated position below 1, and positive ADE by a position above 1 (ADE1; figure 2). Two positions in the same bin indicate the co-occurrence of two ADE types (i.e. the newly introduced ADE2; figure 2). To evaluate the robustness of our findings, we performed these analyses for the global species assemblage with and without singletons (see §3), across geological time periods and at genus level. Furthermore, we implemented two additional analytical approaches which are, however, limited to ADE1 models and do not allow negative and positive ADE to co-occur: (i) a binomial logistic regression between age and extinction; and (ii) ADE-Bayes, a method that, like ADE-NN, estimates the position of age-dependency, but using a Bayesian framework rather than a neural network (see electronic supplementary material, methods [3,11]).

We detected ADE across all 10 time bins, regardless of the extinction regime (i.e. constant, moderate or intense; figure 3a). Negative ADE1 occurred in five time intervals spanning all regimes, whereas ADE2 was found in the remaining five, which were periods of either constant or intense extinction. While four of these periods exhibited negative and positive ADE2, one showed negative ADE2 (i.e. a mix of negative and neutral ADE; figures 2 and 3a). Notably, the distributions of all shape parameters denoting negative ADE were narrower and displayed shorter RMSEs than those exhibiting neutral or positive ADE (figure 3a), suggesting stronger support for negative age-dependency. Furthermore, in three of the four time bins exhibiting negative and positive ADE2, the RMSE crosses 1 in the portion of the data displaying positive age-dependency, casting doubt on the extent to which old species are at high risk of extinction during these time periods (figures 2 and 3a). These results suggest that age is an intrinsic predictor of extinction for neoselachians over the past 145 Myr, with negative age-dependency

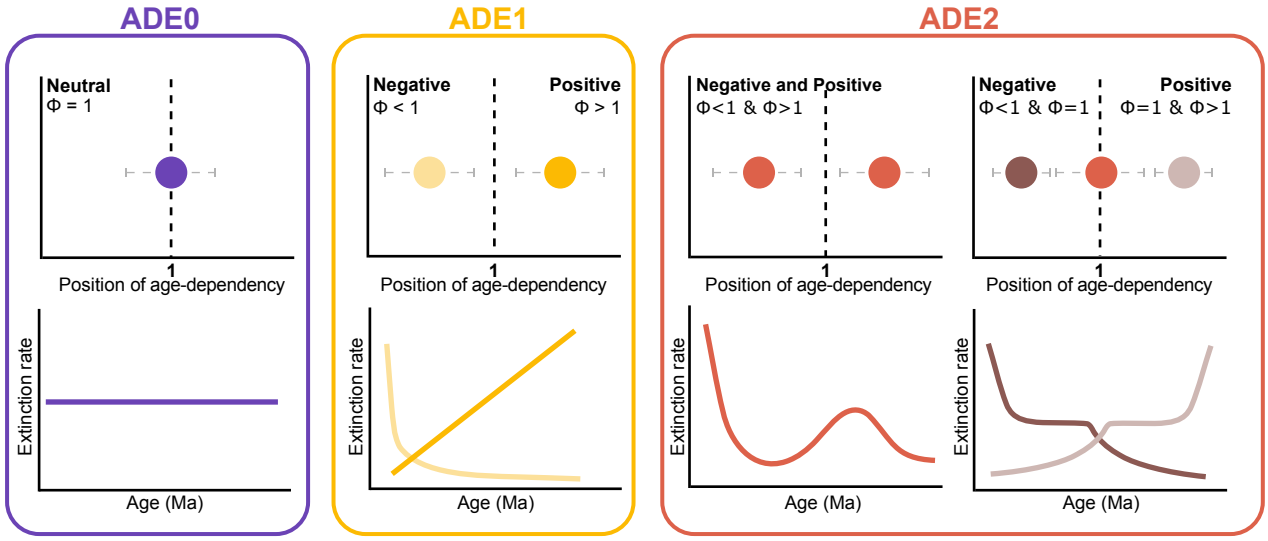

Figure 2. Types of age-dependent extinction (ADE). The position of the predicted value of the Weibull distribution shape parameter (Φ) relative to 1 dictates the ADE type and the corresponding extinction rate relative to lineage age, presented here on the right. Grey horizontal dashed lines represent the prediction error. $\Phi = 1$ represents neutral ADE, $\Phi < 1$ and $\Phi > 1$ corresponds to age-dependency, with $\Phi < 1$ denoting negative ADE, whereby extinction rates decreasing with age, and $\Phi > 1$ denoting positive ADE, with extinction rates increasing with age. ADE2 is newly introduced here, corresponding to two ADE types co-occurring at the same time. Note that in ADE2 (right) the orange marker corresponds to a neutral ADE ($\Phi = 1$), which can co-occur with either a negative or a positive ADE, represented by the light and dark brown markers.

being robustly present across extinction regimes, either on its own (negative ADE1; figure 2), or in combination with neutral or positive dependency (negative ADE2 and negative and positive ADE2; figure 2).

While our main ADE analyses included singletons so that we could capture the full range of longevities (see §3), supplementary analysis excluding them allowed us to assess whether single occurrences, which likely represent short-lived taxa, shifted shape parameters towards negative ADE. We found that negative and positive ADE2 (figure 2) predominated, as it was found in eight of the ten time intervals. Of the remaining two intervals, one showed positive ADE2 and the other neutral ADE (electronic supplementary material, figure S7). However, shape parameters displaying positive dependency are widespread and exhibit large RMSEs. This is especially the case in the Early Cretaceous, the only interval where positive ADE2 was found, suggesting that the ADE type during this time is uncertain (electronic supplementary material, figure S7). These results confirm that the evidence for negative age-dependency is more robust (both as ADE1 and as part of ADE2; figure 2) than for positive dependency (as part of ADE2; figure 2).

Complementary analyses confirm the prevalence of negative ADE in neoselachians, even when extinction regimes are not considered, across different taxonomic resolutions, and when using alternative methods. Indeed, we consistently recovered negative age dependency when using the entire 145 Myr as a single interval, and across geological time periods (i.e. Cretaceous, Palaeogene, and Neogene and Quaternary, the last two merged to maintain relatively similar temporal ranges) at the species and genus levels (electronic supplementary material, figure S8). Furthermore, fitting a binomial logistic regression between age and survival across geological stages (see electronic supplementary material, methods; [11]) recovered a negative correlation (log-odds < 0) in 22 out of 30 stages (73.4%, out of which 12 were statistically significant, $p < 0.05$), indicating that extinction probability decreases with age (electronic supplementary material, figure S9). None of the stages that displayed a positive correlation, and hence potentially positive ADE, was statistically significant ($p > 0.05$). So, despite the binomial logistic regression not allowing positive and negative ADE to co-occur, it nonetheless revealed negative ADE as the prevailing pattern. Taken together, these supplementary analyses confirm that neoselachians have consistently faced higher extinction risk at younger ages throughout their evolutionary history.

Notably, we consistently recovered negative ADE at both the species and genus levels. Genus-level analyses have traditionally been used as a proxy for species-level evolutionary dynamics, particularly in studies limited by incomplete species-level data [63], under the assumption that properties of higher taxa translate into lower taxonomic levels [64]. However, as shown in previous works and exemplified by the diversification patterns recovered here (figure 1; electronic supplementary material, figure S3), genus-level analyses may obscure more nuanced patterns (e.g. [65]). This is particularly relevant for ADE, as its underlying mechanisms differ between species and genera. At the species level, negative ADE is often attributed to ecological traits such as geographical range or specialization [14,15]. However, at the genus level, such traits represent averages across constituent species, potentially oversimplifying biological variation [63]. Instead, ADE patterns at genus level are likely influenced by their diversification potential: genera that continue to diversify reduce their extinction risk over time, whereas those that fail to diversify tend to disappear more quickly, resulting in genera displaying negative ADE even if their constituent species show neutral ADE [21]. Species-level analyses therefore provide more direct and biologically meaningful insights into ADE, even if they represent morphospecies rather than biological species. Our finding of persistent negative ADE across both species and genera underscores the role of age as an intrinsic predictor of extinction in neoselachians, regardless of the underlying diversification dynamics.

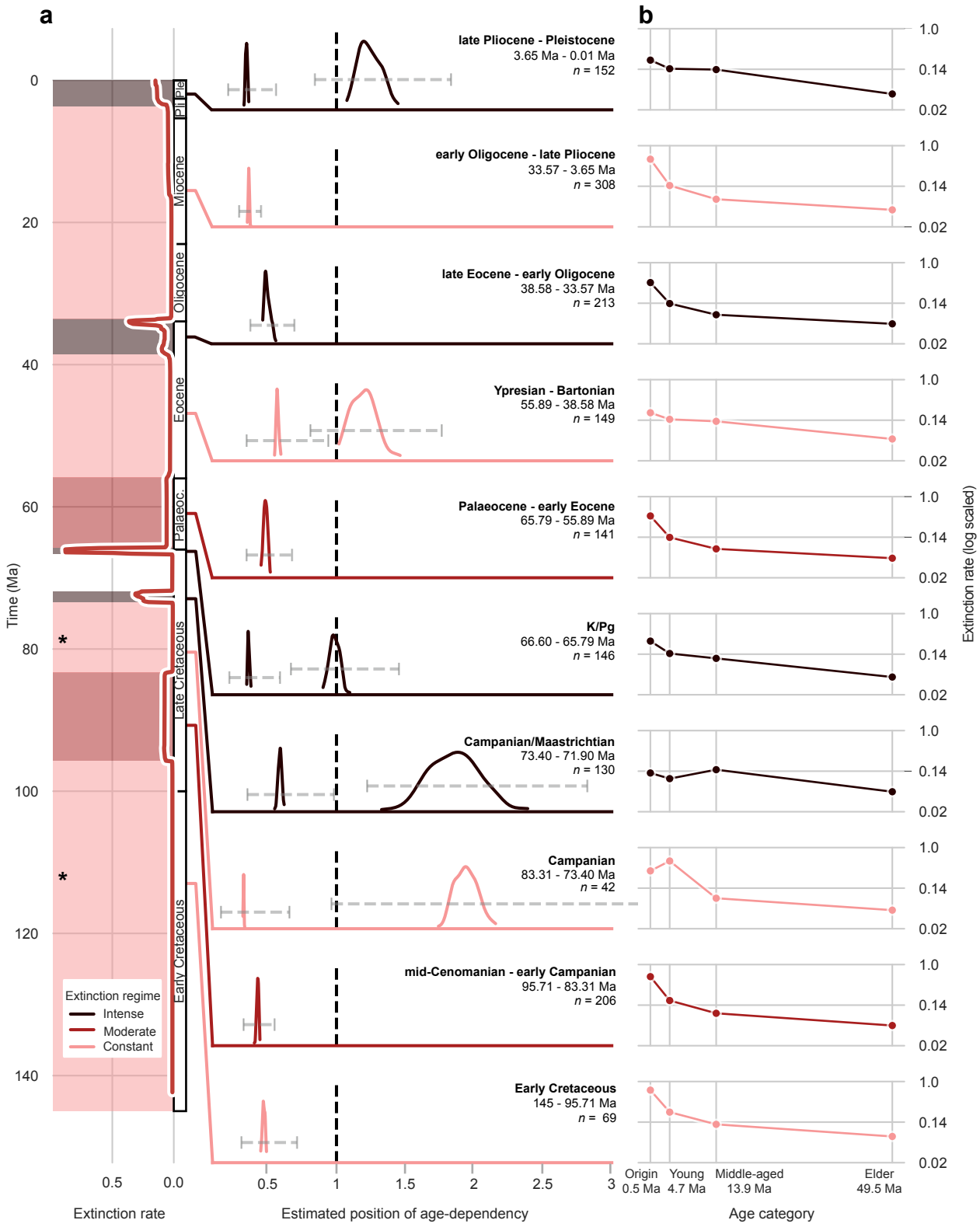

Figure 3. Age-dependent extinction (ADE) of neoselachian species from the Early Cretaceous to the Pleistocene. a) Left: mean extinction rate (red line) defining 10 time bins representing periods of: constant extinction (extinction rate not different from background extinction); moderate extinction (rates ≥3 times the background); and high intensity extinction (rates ≥6 times the background). Time bins marked with an asterisk represent sample sizes lower than 100 (see §3). Palaeoc., Palaeocene; Pli, Pliocene; Ple, Pleistocene. Right: position of age-dependency for each time bin, with horizontal grey dashed lines denoting the root mean square error (RMSE). Black vertical dashed line denotes the value of 1, with positions below 1 marking negative ADE, crossing 1 neutral ADE and above 1 positive ADE. b) Extinction rates were calculated as a function of age across four age categories.

The prevalence of selectivity against young species identified here contrasts sharply with a previous species-level analysis across the K/Pg, which used ADE-Bayes [3,49]. This study reported (i) neutral ADE during the Turonian–Campanian and Palaeocene, and (ii) positive ADE in the Maastrichtian [49]. To determine whether these discrepancies arose from differences in temporal binning, methodology or data, we modelled ADE in these time intervals, applying both ADE-NN and ADE-Bayes to our dataset. ADE-NN revealed negative and neutral ADE (see ADE2 in figure 2) in the Maastrichtian and negative ADE

(see ADE1 in figure 2) in the remaining two time intervals (electronic supplementary material, figure S10), whereas ADE-Bayes indicated positive ADE for all periods (electronic supplementary material, table S2), both diverging from earlier findings. This divergence could result from our new approach, which exposes previously undetected age-dependency patterns. Indeed, ADE-Bayes tends to overestimate shape parameters, making it more likely to estimate neutral or positive ADE when data with poor age resolution are used (specifically over 5 Myr; [4]). This is because, in order to account for low age resolution, ADE-Bayes uses age-randomization within the stratigraphic ranges of fossil occurrences, which can lead to the over-estimation of longevities in short-lived species. As the neoselachian fossil record consists of occurrences with temporal resolutions between *ca* 5 and *ca* 7 Myr on average [34,49], we expect such bias to be present. The ADE-NN approach, on the other hand, directly integrates age uncertainty during model training by including the stratigraphic binning of input data, resulting in a better performance compared with ADE-Bayes [4]. Collectively, these results suggest that the ADE-NN method unveils patterns previously hidden by the limitations of ADE-Bayes, specifically a selective pressure against young neoselachians throughout deep time.

Given the persistent presence of negative ADE over time, we next determined the age at which extinction risk was the greatest for neoselachians. To do so, we first explored species' durations using two approaches (i.e. times of speciation and extinction estimated by PyRate and first and last appearance dates). Our results revealed that despite displaying a left-skewed age-distribution regardless of the method used, neoselachians are long-lived compared with other vertebrates (e.g. [66]), with an average age of *ca* 18 Myr (electronic supplementary material, text and figure S11). We next modelled extinction rates as a function of species' age, based on the estimated Weibull distribution of longevities. We did so for: (i) the global species assemblage; (ii) each time bin across the past 145 Myr representing different extinction regimes; (iii) each extinction regime (i.e. constant, moderate and intense extinction rates); and (iv) each ADE type found here (i.e. negative ADE1 and negative and positive ADE2; figure 2). In the global assemblage, we found extinction rates to be the highest at the earliest age (i.e. 0.5 Myr) and then to decline significantly towards older ages. Specifically, when age was treated as a continuous sequence from 0.5 to 95 Myr, extinction rates declined sharply with increasing longevity before reaching an asymptote, after which they rose again at high longevities (electronic supplementary material, figure S12). A similar pattern emerged when age was categorized as four life-stages—origin (0.5 Myr), young (4.7 Myr), middle-aged (13.9 Myr) and elder (49.5 Myr; figure 4a; see §3). Specifically, (i) extinction rates peak at the origin stage; (ii) then they experience a sharp decline as they approach the young and middle-aged life-stages (three- and twofold declines, respectively); (iii) after this point, extinction rates show a small, 1.6-fold, decrease towards the elder stage, when extinction rates are the lowest (figure 4a). These results collectively suggest that extinction risk is the highest for neoselachians at the beginning of species' existence.

We found a similar trend when examining the 10 time bins representing different extinction regimes over the past 145 Myr, with extinction rates declining from the origin to the elder life-stages (figure 3b). However, deviations were found in the time periods exhibiting ADE2 (figure 2), especially in the three bins displaying negative and positive ADE2 (figure 3b). For instance, during the Campanian, a period of constant extinction, the highest rates take place at the young life-stage, increasing from origin and decreasing again with the following age categories (figure 3b). During the Maastrichtian/Campanian, a period of intense extinction, rates initially decrease between the origin and the young life-stages, then increase towards the middle-age where they reach the highest value and then decrease again as they approach the elder stage (figure 3b). In the late Plio–Pleistocene, a period of intense extinction, rates are very similar across the first three life-stages, particularly between the young and middle-aged stages, with a pronounced decline only towards the elder life-stage (figure 3b). Additionally, the two periods exhibiting negative ADE2, the K/Pg (intense extinction) and the Ypresian–Bartonian (constant extinction), show relatively steady rates between the young and middle-age stages instead of a decline (figure 3b). Moreover, we found extinction risk to be highest at the beginning of species' existence when examining it across extinction regimes and ADE types throughout the entire 145 Myr period (figure 4b,c). Notably, the decline in extinction rates with age is steeper during times of moderate extinction, and less pronounced during times of intense extinction, with the young and middle-aged species experiencing virtually the same level of risk of during times of intense extinction pressures (figure 4b). Overall, our findings collectively demonstrate that age is a persistent intrinsic predictor of extinction in neoselachians through time, with negative age-dependency consistently acting across varying extinction regimes.

Together, our results indicate that negative ADE dominates neoselachian evolutionary history. Indeed, despite some variations in the young and middle-aged life-stages during periods when ADE2 was found, extinction rates generally decrease with age, with no time bin showing high extinction rates at the elder life-stage, even when negative and positive ADE2 are present. Overall, the way extinction risk changes with age in neoselachians is characterized by three main trends: (i) species experience the highest risk during the first 0.5 Myr of age; (ii) extinction risk significantly diminishes as they approach 4 and 14 Myr; (iii) elder species display the lowest extinction risk (figure 4). As such, the first 4 Myr of neoselachians' existence are the most vulnerable, with old age conferring species some level of resilience to extinction.

(c) Conclusions

The diversification history of neoselachians is shaped by multiple phases of elevated extinction that extend beyond the K/Pg. The most significant events occurred during the late Eocene to early Oligocene, and to a lesser extent, the late Plio-Pleistocene. Indeed, we show that neoselachians have not experienced significant speciation in the past 56 Myr, resulting in a diminished diversification throughout much of the Cenozoic. Crucially, our findings reveal that species' age is a persistent predictor of extinction risk over time, with young species consistently facing higher extinction risk than older ones, irrespective of the timing or magnitude of the extinction. While the mechanisms driving age-based selectivity remain unclear and likely involve multiple

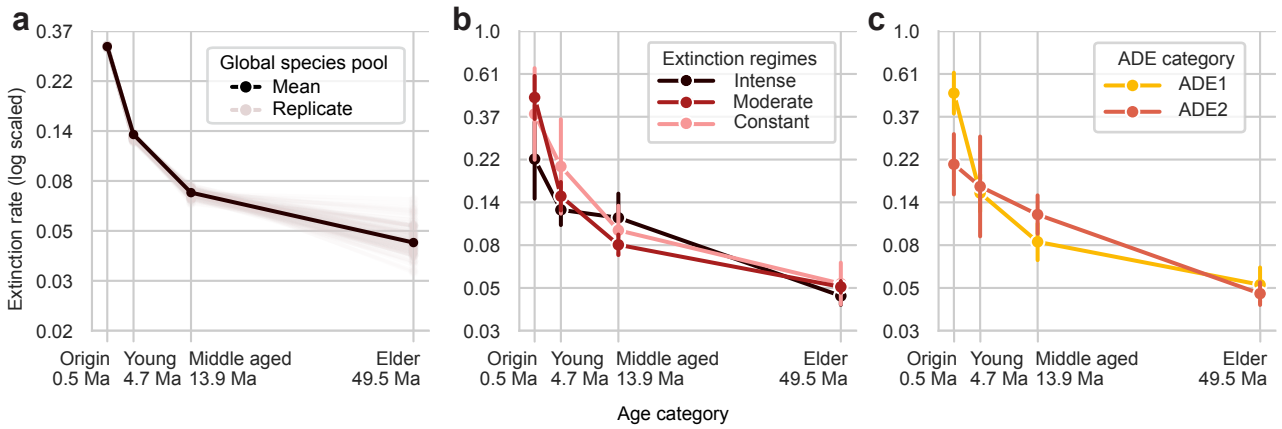

Figure 4. Extinction rate of neoselachian species as a function of age. (a) Extinction rates calculated based on the Weibull shape parameters estimated for the species global assemblage, treating the time widow from 145 to 0.01 Ma as a single time bin. (b) Extinction rates averaged for time bins representing three extinction regimes—intense, moderate and constant. (c) Extinction rates averaged for time bins representing the two ADE types found here—ADE1 and ADE2. Lines extending from each point represent the standard deviation.

factors, we conclude that age-based selectivity is intrinsic to neoselachians. These insights enhance our understanding of the extinction dynamics of sharks and rays, an ecologically important marine clade facing the highest extinction risk among marine vertebrates today.

3. Material and methods

(a) Data

We used the Fossil Neoselachian (FINS) dataset, a highly curated compilation of neoselachian fossil occurrences extracted from literature and the PaleoBiology Database (www.paleobiodb.org), spanning the past 145 Myr (see Data accessibility; [34]). For our analyses, we filtered this dataset based on the following criteria: (i) occurrences identified to species or genus level; (ii) taxonomic nomenclature and age deemed to be valid (for details see [34]); and (iii) occurrences with age ranges of less than or equal to 15 Myr. At the species level, we used 18 328 occurrences representing 1538 taxa, 456 of which had only one occurrence (singletons; electronic supplementary material, data S1). At the genus level, we used 22 638 occurrences representing 500 taxa (electronic supplementary material, data S2). References to the literature from which the data were extracted are available in electronic supplementary material, data S3.

(b) Diversification trajectories

We estimated the extinction, speciation and net diversification rates of neoselachians over the past 145 Myr based on fossil occurrences using PyRate, a Bayesian approach that accounts for preservation and sampling biases (v. 3.1.1; [54]). To account for age uncertainties of fossil occurrences, we resampled the age of each occurrence 10 times, extracting the age from a uniform distribution defined by the minimum and maximum age in each iteration. The subsequent analyses were then repeated for each replicate, and the results were combined to a single posterior sample. The following parameters were simultaneously estimated: (i) preservation rates; (ii) speciation and extinction times, usually extending beyond first and last appearances; and (iii) speciation and extinction rates. We allowed preservation rates to vary across lineages and geological stages. The specific parameters and priors implemented are provided in the code (see [67]). We performed these analyses at the species and genus level. Even though PyRate produces accurate estimates of diversification trajectories even with singleton proportions as high as 30%, we excluded them from our main analyses to minimize biases [53]. However, we performed additional analyses including singletons to assess the robustness of our findings. As another measure of robustness, we estimated the *per capita* extinction, speciation and net diversification rates based on species' first and last appearance dates across geological stages using the *divDyn* R package (see electronic supplementary material, methods; [55,68]).

(c) Age-dependent extinction

Age-dependency was assessed using the ADE-NN method. This framework was first described in Silvestro *et al.* [4], and we further developed it by introducing three new features (v. 3.0). First, we replaced the original categorical classifier used to infer the strength and direction of ADE (strongly negative, negative, neutral, etc.) with a direct estimation of the shape parameter of the Weibull distribution. Second, we introduced a new model with a mixture of two Weibull distributions that infers two shape parameters. Finally, we implemented a classifier to identify the best ADE model.

The ADE-NN 3.0 method comprises two parts: (i) a classifier that assigns the most appropriate model class to a dataset (i.e. ADE0, ADE1 or ADE2; figure 2), and (ii) a regression model that infers the value of the shape parameter(s) (Φ) best describing the distribution of longevities within the dataset, such that:

$$\begin{cases} \Phi = 1, \ \textit{constant extinction} \ (\text{ADE0}) \\ \Phi < 1, \ \textit{negative ADE} \ (\text{ADE1}) \\ \Phi > 1, \ \textit{positive ADE} \ (\text{ADE1}) \\ \Phi_1, \ \Phi_2 \in (0, \infty), \ \text{mixed ADE (ADE2)}, \end{cases}$$

whereby a mixed model results in a distribution of longevities following the combination of two Weibull distributions with parameters Φ1 and Φ2 (figure 2). At the same time, the regression model infers the mean longevity.

Detailed information on the ADE-NN model training and evaluation, and its technical parameters are provided in electronic supplementary material, methods.

(d) ADE-NN implementation

To evaluate age-dependency in neoselachians over the last 145 Myr, we first defined time bins based on extinction rates (i.e. extinction regimes: constant, moderate and intense).

The direction of ADE was then inferred in each time bin by estimating the Weibull shape parameter of longevities distribution using the ADE-NN v. 3.0 method. We included singletons in the main analyses as they may represent truly short-lived taxa, which we aimed to capture. However, singletons may also result from sampling or preservation biases, which can potentially artificially inflate the proportion of short-lived taxa. Therefore, we repeated the analyses without them.

We estimated 100 Φ-values and their RMES in each time bin and plotted their distribution to determine the ADE position (figure 2). The RMSE was calculated by predicting Φ from features simulated while using the sample size of the empirical time bin, and comparing the predicted with the simulated Φ. Thus, the RMSE represents a measure of prediction error of the model, which was found to increase with lower sample sizes (electronic supplementary material, table S3). The narrower the breadth of the RMSE, the higher the prediction power, indicating a strongly supported prediction. In addition to assessing ADE across extinction regimes defined by extinction rates, we assessed it across geological periods and across the entire 145 Myr, without splitting this period into time bins.

We define our ADE mixed model so that the expected longevity of a species follows a mixture of Weibull distributions with shape parameters $\Phi_1, \Phi_2 \in \mathbb{R}^+$and mean set to $m \in \mathbb{R}^+$. From this, we derive the respective scale parameters as $\Psi_i = m/\Gamma(1 + 1/\Phi_i)$ based on the property of a Weibull density function. Given a mixture Weibull function $g(\Phi_1, \Phi_2, \Psi_1, \Psi_2)$, we obtain the ADE rates as:

$$\mu_x = \frac{g(x|\Phi_1, \ \Phi_2, \ \Psi_1, \ \Psi_2)}{1 - \int_0^x g(u|\Phi_1, \ \Phi_2, \ \Psi_1, \ \Psi_2)\mathrm{d}u},$$

where x is the age since origination, and the denominator calculates the probability that the lineage did not go extinct until time x.

We evaluated $g(x)$ and its integral numerically to visualize the extinction rates implied by different parameterizations of our mixture distribution. Note that under the mean, extinction rate equals the inverse of the longevity ($1/m$), as expected under a stochastic birth–death process.

We modelled the extinction rate across a continuous age sequence from 0.1 to 95 Ma, and at four different life-stages representing the time of origination (0.5 Ma), the young life-stage (median of the shortest 1% of longevities, 4.4 Ma), the middle-aged stage (median of overall longevities, 13.8 Ma) and the elder stage (median of the longest 1% of longevities, 49.4 Ma).

To evaluate the robustness of our results, we estimated ADE using ADE-Bayes [3] and a binomial logistic regression between age and extinction across geological stages (see electronic supplementary material, methods; [11]).

Ethics. This work did not require ethical approval from a human subject or animal welfare committee.

Data accessibility. The data used in this study were obtained from the Fossil Neoselachian (FINS) dataset, which is openly accessible from the Zenodo repository [69]. Version v. 1 of the dataset was used here. We filtered these data (see §3) for our analyses. These filtered raw data are included in electronic supplementary material, data S1 and S2, and the references associated with these data are presented in electronic supplementary material, data S3. All code and data used for the analyses are openly accessible via the Zenodo repository [67], including a ReadMe file describing the usage of each script. Supplementary material is available online [70].

Declaration of AI use. We have not used AI-assisted technologies in creating this article.

Authors' contributions. K.K.: data curation, formal analysis, methodology, visualization, writing—original draft; D.S.: formal analysis, methodology, visualization, writing—review and editing; G.H.M.: visualization, writing—review and editing; J.A.V.: data curation, writing—review and editing; C.P.: conceptualization, methodology, visualization, writing—original draft.

All authors gave final approval for publication and agreed to be held accountable for the work performed herein.

Conflict of interest declaration. We declare we have no competing interests.

Funding. This work was supported by the Swiss National Science Foundation (PRIMA_185798 to C.P.), the Swedish Foundation for Strategic Environmental Research (MISTRA) under the BIOPATH research programme (F 2022/1448 to D.S.), and ETH Zurich (D.S.).

Acknowledgements. We thank the two anonymous reviewers for their constructive feedback, which allowed us to improve the manuscript significantly.

References

1. Doran NA, Arnold AJ, Parker WC, Huffer FW. 2006 Is extinction age dependent? *Palaios* **21**, 571–579. (doi:10.2110/palo.2006.p06-055r)

2. Smits PD. 2015 Expected time-invariant effects of biological traits on mammal species duration. *Proc. Natl Acad. Sci. USA* **112**, 13015–13020. (doi:10.1073/pnas.1510482112)
3. Hagen O, Andermann T, Quental TB, Antonelli A, Silvestro D. 2018 Estimating age-dependent extinction: contrasting evidence from fossils and phylogenies. *Syst. Biol*. **67**, 458–474. (doi:10.1093/sysbio/syx082)
4. Silvestro D *et al*. 2020 A 450 million years long latitudinal gradient in age-dependent extinction. *Ecol. Lett*. **23**, 439–446. (doi:10.1111/ele.13441)
5. Van Valen L. 1973 A new evolutionary law. *Evol. Theory* **1**, 1–30.
6. Pearson PN. 1995 Investigating age-dependency of species extinction rates using dynamic survivorship analysis. *Hist. Biol*. **10**, 119–136. (doi:10.1080/10292389509380516)
7. Boyajian G, Lutz T. 1992 Evolution of biological complexity and its relation to taxonomic longevity in the Ammonoidea. *Geology* **20**, 983–986. (doi:10.1130/0091-7613(1992)0202.3.co;2)
8. Crampton JS, Cooper RA, Sadler PM, Foote M. 2016 Greenhouse–icehouse transition in the Late Ordovician marks a step change in extinction regime in the marine plankton. *Proc. Natl Acad. Sci. USA* **113**, 1498–1503. (doi:10.1073/pnas.1519092113)
9. Ezard THG, Quental TB, Benton MJ. 2016 The challenges to inferring the regulators of biodiversity in deep time. *Phil. Trans. R. Soc. B* **371**, 20150216. (doi:10.1098/rstb.2015.0216)
10. Januario M, Quental TB. 2021 Re-evaluation of the 'law of constant extinction' for ruminants at different taxonomical scales. *Evolution* **75**, 656–671. (doi:10.1111/evo.14177)
11. Finnegan S, Payne JL, Wang SC. 2008 The Red Queen revisited: reevaluating the age selectivity of Phanerozoic marine genus extinctions. *Paleobiology* **34**, 318–341. (doi:10.1666/07008.1)
12. Johnson MTJ, Fitzjohn RG, Smith SD, Rausher MD, Otto SP. 2011 Loss of sexual recombination and segregation is associated with increased diversification in evening primroses. *Evolution* **65**, 3230–3240. (doi:10.1111/j.1558-5646.2011.01378.x)
13. Balmford A. 1996 Extinction filters and current resilience: the significance of past selection pressures for conservation biology. *Trends Ecol. Evol*. **11**, 193–196. (doi:10.1016/0169-5347(96)10026-4)
14. Liow LH. 2007 Lineages with long durations are old and morphologically average: an analysis using multiple datasets. *Evolution* **61**, 885–901. (doi:10.1111/j.1558-5646.2007.00077.x)
15. Foote M, Crampton JS, Beu AG, Cooper RA. 2008 On the bidirectional relationship between geographic range and taxonomic duration. *Paleobiology* **34**, 421–433. (doi:10.1666/08023.1)
16. Jablonski D. 2008 Species selection: theory and data. *Annu. Rev. Ecol. Evol. Syst*. **39**, 501–524. (doi:10.1146/annurev.ecolsys.39.110707.173510)
17. Liow LH, Skaug HJ, Ergon T, Schweder T. 2010 Global occurrence trajectories of microfossils: environmental volatility and the rise and fall of individual species. *Paleobiology* **36**, 224–252. (doi:10.1666/08080.1)
18. Foote M, Miller AI. 2013 Determinants of early survival in marine animal genera. *Paleobiology* **39**, 171–192. (doi:10.1666/12028)
19. Anstey RL. 1978 Taxonomic survivorship and morphologic complexity in Paleozoic bryozoan genera. *Paleobiology* **4**, 407–418. (doi:10.1017/s0094837300006151)
20. Jones DS, Nicol D. 1986 Origination, survivorship, and extinction of rudist taxa. *J. Paleontol*. **60**, 107–115. (doi:10.1017/s0022336000021557)
21. Raup DM. 1985 Mathematical models of cladogenesis. *Paleobiology* **11**, 42–52. (doi:10.1017/s0094837300011386)
22. Ezard THG, Aze T, Pearson PN, Purvis A. 2011 Interplay between changing climate and species' ecology drives macroevolutionary dynamics. *Science* **332**, 349–351. (doi:10.1126/science.1203060)
23. Pearson PN. 1992 Survivorship analysis of fossil taxa when real-time extinction rates vary: the Paleogene planktonic Foraminifera. *Paleobiology* **18**, 115–131. (doi:10.1017/s0094837300013920)
24. Boyajian GE. 1991 Taxon age and selectivity of extinction. *Paleobiology* **17**, 49–57. (doi:10.1017/s0094837300010344)
25. Condamine FL, Romieu J, Guinot G. 2019 Climate cooling and clade competition likely drove the decline of lamniform sharks. *Proc. Natl Acad. Sci. USA* **116**, 20584–20590. (doi:10.1073/pnas.1902693116)
26. Pires MM, Rankin BD, Silvestro D, Quental TB. 2018 Diversification dynamics of mammalian clades during the K–Pg mass extinction. *Biol. Lett*. **14**, 20180458. (doi:10.1098/rsbl.2018.0458)
27. Longrich NR, Tokaryk T, Field DJ. 2011 Mass extinction of birds at the Cretaceous–Paleogene (K–Pg) boundary. *Proc. Natl Acad. Sci. USA* **108**, 15253–15257. (doi:10.1073/pnas.1110395108)
28. Brusatte SL *et al*. 2015 The extinction of the dinosaurs. *Biol. Rev*. **90**, 628–642. (doi:10.1111/brv.12128)
29. Solórzano A, Núñez-Flores M, Inostroza-Michael O, Hernández CE. 2020 Biotic and abiotic factors driving the diversification dynamics of Crocodylia. *Palaeontology* **63**, 415–429. (doi:10.1111/pala.12459)
30. Demetrius L. 1978 Adaptive value, entropy and survivorship curves. *Nature* **275**, 213–214. (doi:10.1038/275213a0)
31. Maisey JG, Naylor GJP, Ward DJ. 2004 Mesozoic elasmobranchs, neoselachian phylogeny and the rise of modern elasmobranch diversity. In *Mesozoic fishes 3 – systematics, paleoenvironments and biodiversity* (eds G Arratia, A Tintori), pp. 17–56. Munich, Germany: Verlag Dr. Friedrich Pfeil.
32. Dillon EM, Pimiento C. 2025 Aligning paleobiological research with conservation priorities using elasmobranchs as a model. *Paleobiology* **51**, 112–131. (doi:10.1017/pab.2024.11)
33. Cappetta H. 2012 *Handbook of paleoichthyology: chondrichthyes*. vol. **3E**. Munich, Germany: Verlag Dr. Friedrich Pfeil.
34. Kocáková K, Villafaña JA, Gardiner A, Mathes GH, Pimiento C. FINS - a global occurrence dataset of fossil neoselachians from the Cretaceous to the Quaternary. *bioRxiv* 2025.11.21.689757. (doi:10.1101/2025.11.21.689757)
35. Myers RA, Baum JK, Shepherd TD, Powers SP, Peterson CH. 2007 Cascading effects of the loss of apex predatory sharks from a coastal ocean. *Science* **315**, 1846–1850. (doi:10.1126/science.1138657)
36. Shimada K, Ward D. 2016 The oldest fossil record of the megamouth shark from the late Eocene of Denmark, and comments on the enigmatic megachasmid origin. *Acta Palaeontol. Pol.* **61**, 839–845. (doi:10.4202/app.00248.2016)
37. Weigmann S. 2016 Annotated checklist of the living sharks, batoids and chimaeras (Chondrichthyes) of the world, with a focus on biogeographical diversity. *J. Fish Biol*. **88**, 837–1037. (doi:10.1111/jfb.12874)
38. Navia AF, Mejía-Falla PA, López-García J, Giraldo A, Cruz-Escalona VH. 2017 How many trophic roles can elasmobranchs play in a marine tropical network? *Mar. Freshw. Res*. **68**, 1342. (doi:10.1071/mf16161)
39. Ebert DA, Dando M, Fowler S. *Sharks of the world: a complete guide*. Princeton, NJ: Princeton University Press. See http://www.jstor.org/stable/10.2307/j.ctv1574pqp.
40. Cooper JA *et al*. 2022 The extinct shark *Otodus megalodon* was a transoceanic superpredator: inferences from 3D modeling. *Sci. Adv*. **8**, eabm9424. (doi:10.1126/sciadv.abm9424)
41. Cooper JA, Pimiento C. 2024 The rise and fall of shark functional diversity over the last 66 million years. *Glob. Ecol. Biogeogr*. **33**, e13881. (doi:10.1111/geb.13881)
42. Paramo J, Wiff R, González R. 2021 A matter of size: the population structure of the smallest known living shark, *Etmopterus perryi* (Springer & Burgess, 1985), from deep waters off the Colombian Caribbean coast. *J. Fish Biol*. **99**, 755–764. (doi:10.1111/jfb.14755)

43. Kriwet J, Benton M. 2004 Neoselachian (Chondrichthyes, Elasmobranchii) diversity across the Cretaceous–Tertiary boundary. *Palaeogeogr. Palaeoclimatol. Palaeoecol*. **214**, 181–194. (doi:10.1016/s0031-0182(04)00420-1)
44. Kriwet J, Klug S. 2008 Diversity and biogeography patterns of Late Jurassic neoselachians (Chondrichthyes: Elasmobranchii). *Geol. Soc. Lond. Spec. Publ*. **295**, 55–70. (doi:10.1144/sp295.5)
45. Kriwet J, Kiessling W, Klug S. 2009 Diversification trajectories and evolutionary life-history traits in early sharks and batoids. *Proc. R. Soc. B* **276**, 945–951. (doi:10.1098/rspb.2008.1441)
46. Guinot G, Adnet S, Cappetta H. 2012 An analytical approach for estimating fossil record and diversification events in sharks, skates and rays. *PLoS One* **7**, e44632. (doi:10.1371/journal.pone.0044632)
47. Villafaña JA, Rivadeneira MM. 2014 Rise and fall in diversity of Neogene marine vertebrates on the temperate Pacific coast of South America. *Paleobiology* **40**, 659–674. (doi:10.1666/13069)
48. Brée B, Condamine FL, Guinot G. 2022 Combining palaeontological and neontological data shows a delayed diversification burst of carcharhiniform sharks likely mediated by environmental change. *Scient. Rep*. **12**, 21906. (doi:10.21203/rs.3.rs-1930062/v1)
49. Guinot G, Condamine FL. 2023 Global impact and selectivity of the Cretaceous-Paleogene mass extinction among sharks, skates, and rays. *Science* **379**, 802–806. (doi:10.1126/science.abn2080)
50. Villafaña JA, Rivadeneira MM, Pimiento C, Kriwet J. 2023 Diversification trajectories and paleobiogeography of Neogene chondrichthyans from Europe. *Paleobiology* **49**, 329–341. (doi:10.1017/pab.2022.40)
51. Pimiento C, Griffin JN, Clements CF, Silvestro D, Varela S, Uhen MD, Jaramillo C. 2017 The Pliocene marine megafauna extinction and its impact on functional diversity. *Nat. Ecol. Evol*. **1**, 1100–1106. (doi:10.1038/s41559-017-0223-6)
52. Sibert EC, Rubin LD. 2021 An early Miocene extinction in pelagic sharks. *Science* **372**, 1105–1107. (doi:10.1126/science.aaz3549)
53. Silvestro D, Schnitzler J, Liow LH, Antonelli A, Salamin N. 2014 Bayesian estimation of speciation and extinction from incomplete fossil occurrence data. *Syst. Biol*. **63**, 349–367. (doi:10.1093/sysbio/syu006)
54. Silvestro D, Salamin N, Schnitzler J. 2014 PyRate: a new program to estimate speciation and extinction rates from incomplete fossil data. *Methods Ecol. Evol*. **5**, 1126–1131. (doi:10.1111/2041-210x.12263)
55. Kocsis AT, Reddin CJ, Alroy J, Kiessling W. 2019 The R package divDyn for quantifying diversity dynamics using fossil sampling data. *Methods Ecol. Evol* **10**, 735–743. (doi:10.1101/423780)
56. Guinot G, Cavin L. 2016 'Fish' (Actinopterygii and Elasmobranchii) diversification patterns through deep time. *Biol. Rev*. **91**, 950–981. (doi:10.1111/brv.12203)
57. Ikejiri T, Lu Y, Zhang B. 2020 Two-step extinction of Late Cretaceous marine vertebrates in northern Gulf of Mexico prolonged biodiversity loss prior to the Chicxulub impact. *Scient. Rep*. **10**, 4169. (doi:10.1038/s41598-020-61089-w)
58. Callegaro S, Baker DR, Renne PR, Melluso L, Geraki K, Whitehouse MJ, De Min A, Marzoli A. 2023 Recurring volcanic winters during the latest Cretaceous: sulfur and fluorine budgets of Deccan Traps lavas. *Sci. Adv*. **9**, eadg8284. (doi:10.1126/sciadv.adg8284)
59. Prothero DR. 1994 The Late Eocene-Oligocene extinctions. *Annu. Rev. Earth Planet. Sci*. **22**, 145–165. (doi:10.1146/annurev.ea.22.050194.001045)
60. Pimiento C, Benton MJ. 2020 The impact of the Pull of the Recent on extant elasmobranchs. *Palaeontology* **63**, 369–374. (doi:10.1111/pala.12478)
61. Silvestro D, Antonelli A, Salamin N, Meyer X. Improved estimation of macroevolutionary rates from fossil data using a Bayesian framework. *Paleontology* 546–570. (doi:10.1101/316992)
62. Černý D, Madzia D, Slater GJ. 2021 Empirical and methodological challenges to the model-based inference of diversification rates in extinct clades. *Syst. Biol*. **71**, 153–171. (doi:10.1093/sysbio/syab045)
63. Hendricks JR, Saupe EE, Myers CE, Hermsen EJ, Allmon WD. 2014 The generification of the fossil record. *Paleobiology* **40**, 511–528. (doi:10.1666/13076)
64. Jablonski D. 2007 Scale and hierarchy in macroevolution. *Palaeontology* **50**, 87–109. (doi:10.1111/j.1475-4983.2006.00615.x)
65. Lloyd GT, Young JR, Smith AB. 2012 Taxonomic structure of the fossil record is shaped by sampling bias. *Syst. Biol*. **61**, 80–89. (doi:10.1093/sysbio/syr076)
66. Prothero DR. 2014 Species longevity in North American fossil mammals. *Integr. Zool*. **9**, 383–393. (doi:10.1111/1749-4877.12054)
67. Kocakova K, Silvestro D, Mathes GH, Villafaña Navea JA, Pimiento C. 2025 Data from: Global extinction events and persistent age-dependency in sharks and rays over the past 145 million years. Zenodo. (doi:10.5281/zenodo.17475049)
68. R Core Team. *R: a language and environment for statistical computing*. Vienna, Austria: R Foundation for Statistical Computing. See http://www.R-project.org/.
69. Kocakova K, Villafaña Navea JA, Gardiner A, Mathes GH, Pimiento C. 2025 FINS: Fossil Neoselachian dataset. Zenodo (doi:10.5281/zenodo.17371411)
70. Kocáková K, Silvestro D, Mathes GH, Villafaña JA, Pimiento C. 2025 . Supplementary Material from: Global Extinction Events and Persistent Age-Dependency in Sharks and Rays over the Past 145 Million Years. Figshare. (doi:10.6084/m9.figshare.c.8142777)